Supplementary Information for

Dual-Layered Percolative Networks of Photoactive Materials and Elastomers for Highly-Stretchable, Efficient Organic Photovoltaics with Strain-Induced Power Enhancement up to 60% Strain

Jin-Woo Lee[†,a], *Jongmin Oh*[†,a], *Won Jung Kang*[†,b], *Eun Sung Oh*[b], *Seungbok Lee*[c], *Inwoo Lee*[a], *Jimin Park*[a], *Jung-Yong Lee*[c], *Taek-Soo Kim*[b,*], *and Bumjoon J. Kim*[a,*]

[a] Department of Chemical and Biomolecular Engineering, Korea Advanced Institute of Science and Technology (KAIST), Daejeon 34141, Republic of Korea

[b] Department of Mechanical Engineering, KAIST, Daejeon 34141, Republic of Korea

[c] School of Electrical Engineering, KAIST, Daejeon 34141, Republic of Korea

[*]All correspondence should be addressed to B. J. K. (E-mail: bumjoonkim@kaist.ac.kr) and T.-S. K. (E-mail: tskim1@kaist.ac.kr).

Main abbreviations

OSC: organic solar cell

IS-OSC: intrinsically stretchable organic solar cell

PCE: power conversion efficiency

P_D: polymer donor

SMA: small-molecule acceptor

SEBS: styrene-ethylene-butylene-styrene

COS: crack-onset strain

DLP: dual-layered percolative

***J–V*:** current density-voltage

V_{oc}: open-circuit voltage

J_{sc}: short-circuit current density

FF: fill-factor

D18: Poly[(2,6-(4,8-bis(5-(2-ethylhexyl-3-fluoro)thiophen-2-yl)-benzo[1,2-*b*:4,5-*b*']dithiophene))-*alt*-5,5'-(5,8-bis(4-(2-butyloctyl)thiophen-2-yl)dithieno[3',2':3,4;2",3":5,6]benzo[1,2-*c*][1,2,5]thiadiazole)]

PM6: Poly[(2,6-(4,8-bis(5-(2-ethylhexyl)-4-fluorothiophen-2-yl)-benzo[1,2-*b*:4,5-*b*']dithiophene))-*alt*-(5,5-(1',3'-di-2-thienyl-5',7'-bis(2-ethylhexyl)benzo[1',2'-*c*:4',5'-*c*']dithiophene-4,8-dione))]

L8-BO: *2,2′-((2Z**,*2′Z*)-((12,13-bis(2-butyloctyl)-3,9-diundecyl-12,13-dihydro-[1,2,5]thiadiazolo[3,4-*e*]thieno[2‴:4,5]thieno[2′,3′:4,5]pyrrolo[3,2-*g*]thieno[2′,3′:4,5]thieno[3,2-*b*]indole-2,10-diyl)bis(methanylylidene))bis(5,6-difluoro-3-oxo-1*H*-indene-2,1(3*H*)-diylidene))dimalononitrile

Experimental Section

***Materials*:** 2,2'-((2*Z*,2'*Z*)-((12,13-bis(2-ethylhexyl)-3,9-(2-butyloctyl)-12,13-dihydro-[1,2,5]thiadiazolo[3,4-*e*]thieno[2",3'':4',5']thieno[2',3':4,5]pyrrolo[3,2-*g*]thieno[2',3':4,5]thieno[3,2-*b*]indole-2,10-diyl)bis(methanylylidene))bis(5,6-difluoro-3-oxo-2,3-dihydro-1*H*-indene-2,1-diylidene))dimalononitrile (L8-BO) was purchased from Derthon Inc. Polystyrene-block-poly(ethylene-ran-butylene)-block-polystyrene (SEBS) was synthesized according to the previously reported procedure.[1] Poly[(9,9-bis(3′-((*N*,*N*-dimethyl)-*N*-ethylammonium)propyl)-2,7-fluorene)-*alt*-5,5′-bis(2,2′-thiophene)-2,6-naphthalene-1,4,5,8-tetracaboxylic-*N*,*N*′-di(2-ethylhexyl)imide]dibromide (PNDIT-F3N-Br) was synthesized according to the reported method.[2] Poly[(2,6-(4,8-bis(5-(2-ethylhexyl-3-fluoro)thiophen-2-yl)-benzo[1,2-b:4,5-b']dithiophene))-alt-5,5'-(5,8-bis(4-(2-butyloctyl)thiophen-2-yl)dithieno[3',2':3,4;2",3":5,6]benzo[1,2-c][1,2,5]thiadiazole)] (D18) and poly[(2,6-(4,8-bis(5-(2-ethylhexyl-3-fluoro)thiophen-2-yl)-benzo[1,2-b:4,5-b']dithiophene))-*alt*-(5,5-(1',3'-di-2-thienyl-5',7'-bis(2-ethylhexyl)benzo[1',2'-c:4',5'-c']dithiophene-4,8-dione) (PM6) were synthesized following the previously reported synthetic steps.[3, 4]

Characterizations: A UV-1800 spectrophotometer was used for the UV−Vis absorption spectra. The molecular weight of the polymers was estimated by high-temperature gel permeation chromatography (GPC) at 140 °C using 1,2,4-trichlorobenzene as an eluent, which was calibrated using polystyrene standards. CV curves were obtained using a common three-electrode system from an EG and G Parc model 273 Å system.

The differential scanning calorimetry (DSC) profiles were obtained by TA Instruments DSC 25 with heating and cooling rates of 10 ℃ min^{-1} from -70 to 180 °C. The atomic force microscopy (AFM) images were measured by NX10 from Park Systems. Grazing incidence wide-angle X-ray scattering (GIXS) measurements were conducted at the Pohang Accelerator Laboratory (beamline 3C, Republic of Korea), with incidence angles between 0.12 – 0.14°. Correlation length (L_c) values of the crystallites were calculated using the Scherrer equation:

$$L_c = \frac{2\pi K}{\Delta_q}$$

(K (shape factor) = 0.9 and Δ_q = full width half maximum (FWHM) of the scatterings)

The resonant soft X-ray scattering (RSoXS) experiment was performed at beamline 11.0.1.2 in the S11 Advanced Light Source (United States). Blend films for the RSoXS measurement were prepared on a 100 nm-thick, 1.0 mm × 1.0 mm Si_3N_4 membrane supported by a 200-μm thick, 5 mm × 5 mm silicon frame (Norcada Inc.). The domain size of a blend film was approximated to be half of the domain spacing (domain spacing= $2\pi q_{peak}^{-1}$) from the RSoXS profile. The relative domain purity was estimated as the relative ratio of square-root of the integrated scattering intensity in the Iq^2 vs. q plot. Bruker Avance III HD Nanobay (9.4 T) 400 MHz spectrometer was used to measure ^{1}H NMR spectra. The chemical shifts in the spectra have units of ppm. Cyclic voltammetry (CV) was performed using a EG and G Parc model 273 Å potentiostat/galvanostat

system in a 0.1 M tetrabutylammonium perchlorate solution with nitrogen degassed anhydrous acetonitrile as the supporting electrolyte, at a scan rate of 50 mV s^{-1}. A glassy carbon electrode was used as the working electrode. A platinum wire was used as the counter electrode, and an Ag/AgCl electrode was used as the reference electrode. The redox couple ferricenium/ferrocene was used as external standard. HOMO and LUMO energy levels were estimated from cyclic voltammetry: E_{HOMO} (eV) = $-(E_{onset}^{ox.} - E_{onset}^{Fc/Fc+}) + E_{HOMO}^{Fc}$; E_{LUMO} (eV) = $-(E_{onset}^{red.} - E_{onset}^{Fc/Fc+}) + E_{HOMO}^{Fc}$; $E_{onset}^{Fc/Fc+}$= 0.44 eV, E_{HOMO}^{Fc}= −4.8 eV.

Pseudo free-standing tensile test: The films were prepared with the same condition as that used for the OSC fabrications. The films were spin-casted onto Poly(4-styrenesulfonic acid)-coated glass substrates, and cut into a dog-bone shape by a femtosecond laser. Then, the films were floated onto the water surface, and attached to the grips by van der Waals forces. The strain was applied at a fixed strain rate (0.8×10^{-3} s^{-1}), and the tensile load values were measured by a load cell with high resolution (LTS-50GA, KYOWA, Japan). Elastic modulus was calculated using the least square method for the slope of the linear region of the stress–strain curve within 1.0% strain. The crack-onset strain (COS) of a thin film was determined as the strain value that the tensile load starts to decrease rapidly by cracking.

OSC Fabrication and Characterization: The OSCs with a normal architecture (ITO/ PEDOT:PSS/active layer/PNDIT-F3N-Br/Ag) were prepared with the following procedures. ITO-coated glass substrates were treated by ultrasonication with deionized water, acetone, and isopropyl alcohol. Then, the ITO substrates were dried for 6 h in an oven (70 °C) at an ambient pressure, and then plasma treated for 10 min. Spin-coating of the PEDOT:PSS solution (Clevios,

AI4083) was performed at 3300 rpm for 30 sec onto the ITO substrates. Then, the film/substrate was annealed in the air at 150 °C for 15 min before transferring into an N_2-filled glovebox. The active layer solution, prepared under optimized conditions, was spin-coated onto the PEDOT:PSS/ITO substrate to form an active layer with a thickness of 130–180 nm. Specifically, D18 and SEBS polymers were separately dissolved in chlorobenzene at 100°C with 1-chloronaphthalene (0.5 v/v) additives and then mixed at different composition ratios to yield $D18_{1.0-x}$:$SEBS_x$ solutions. Meanwhile, PM6 and L8-BO were dissolved separately in carbon tetrachloride at 80°C with 3,5-dichlorobromobenzene (10 mg mL^{-1}) additive, and mixed at different composition ratios to produce $PM6_x$:$L8\text{-}BO_{1-x}$ solutions. The $D18_{1.0-x}$:$SEBS_x$ solutions were first spin-coated onto the PEDOT:PSS layer to form the bottom layers with a thickness of 80–120 nm and annealed at 80°C for 5 min. The $PM6_x$:$L8\text{-}BO_{1-x}$ solutions were then spin-coated onto the $D18_{1.0-x}$:$SEBS_x$ layers to form the top layers with a thickness of 50–60 nm. Afterward, the samples were annealed at 80°C for 5 min and dried under high vacuum (< 10^{-6} Torr) for 1 h. PNDITF3N-Br in methanol (1 mg mL^{-1}) was then spin-coated with the condition of 3000 rpm for 30 sec. Finally, Ag (120 nm) was deposited under high vacuum (~10^{-6} Torr) in an evaporation chamber. Optical microscopy (OM) was used to measure the exact photoactive area of the mask (0.06 cm^2). Keithley 2400 SMU instrument was used to measure the PCE values under an Air Mass 1.5 G solar simulator (100 mW cm^{-2}, solar simulator: K201 LAB55, McScience), satisfying the Class AAA, ASTM Standards. K801SK302 of McScience was used as a standard silicon reference cell to calibrate the exact solar intensity. The average measurement duration for each OSC device was 5.9 s. K3100 IQX, McScience Inc. instrument was used to analyze the EQE spectra, equipped with a monochromator (Newport) and an optical chopper (MC 2000 Thorlabs).

IS-OSC Fabrication: Normal-type IS-OSCs with a device configuration (thermoplastic polyurethanes (TPU)/modified PH1000/AI4083/photoactive layers/PNDIT-F3N-Br/eutectic gallium indium (EGaIn)) were fabricated. The modified PH1000 solution was prepared to contain 5 vol% of dimethyl sulfoxide (DMSO) (to increase the electrical conductivity of PH1000), 2 vol% of polyethylene glycol (PEG) (to improve mechanical stretchability), 0.5 vol% of Zonyl fluoro surfactant (FS-30) (to enhance the surface wettability), and 0.5 vol% of (3-glycidyloxypropyl)trimethoxysilane (GOPS) (to enhance mechanical stretchability). Then the solution was spin-coated at 1200 rpm for 40 s on the plasma-treated TPU substrate and treated for 20 min at 100 °C in air. Next, AI4083 (with FS-30 0.5 vol%) hole transporting layer was spin-coated at 2500 rpm for 40 s on the PH1000/TPU substrate and dried at 100 °C for 20 min. Subsequently, the photoactive layers were spin-coated with the same condition as that used for the OSC fabrication on the rigid ITO/glass substrate. Then, the PNDIT-F3N-Br solution in methanol (1 mg mL^{-1}) was spin-coated at 3000 rpm for 40 s to yield a 5 nm thick electron transporting layer on the active layer. Finally, EGaIn liquid metal was sprayed on the layer through a deposition mask. The photovoltaic performances of IS-OSCs were tested by the same instruments as those used for the measurement of the performances of the rigid OSCs.

Supplementary Figures and Tables

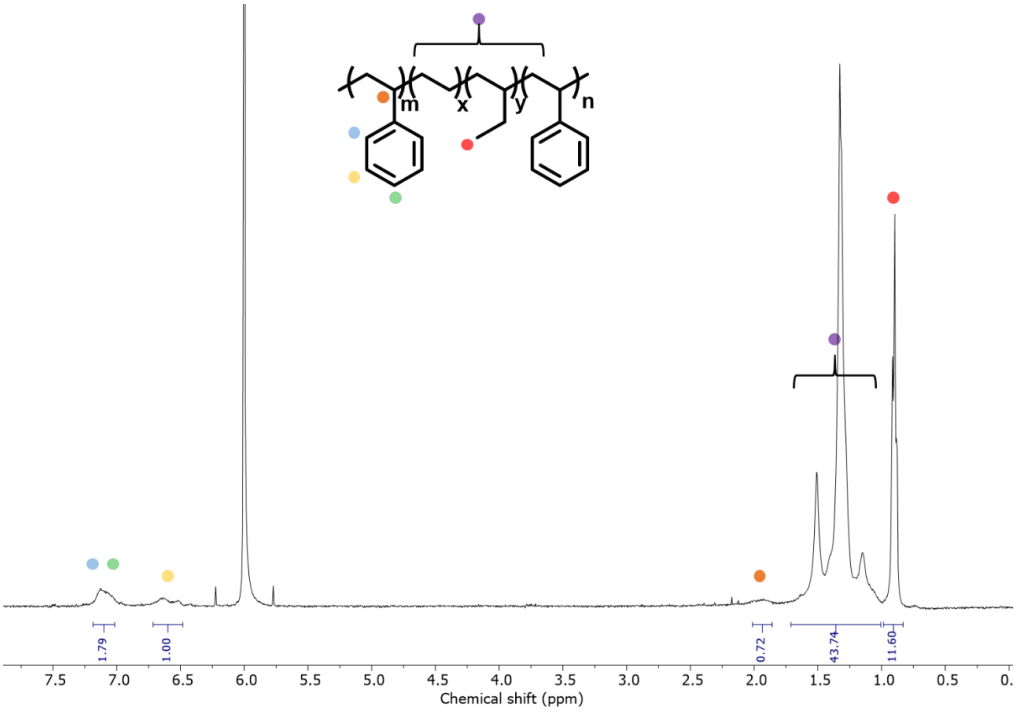

Fig. S1. ^{1}H NMR spectra of SEBS.

Table S1. Molecular weight information of D18, PM6, and SEBS polymers measured by GPC at 140 °C using 1,2,4-trichlorobenzene as eluent.

Polymer	M_n (kg mol^{-1})	$Đ$
D18	62	2.0
PM6	53	4.8
SEBS	164	1.1

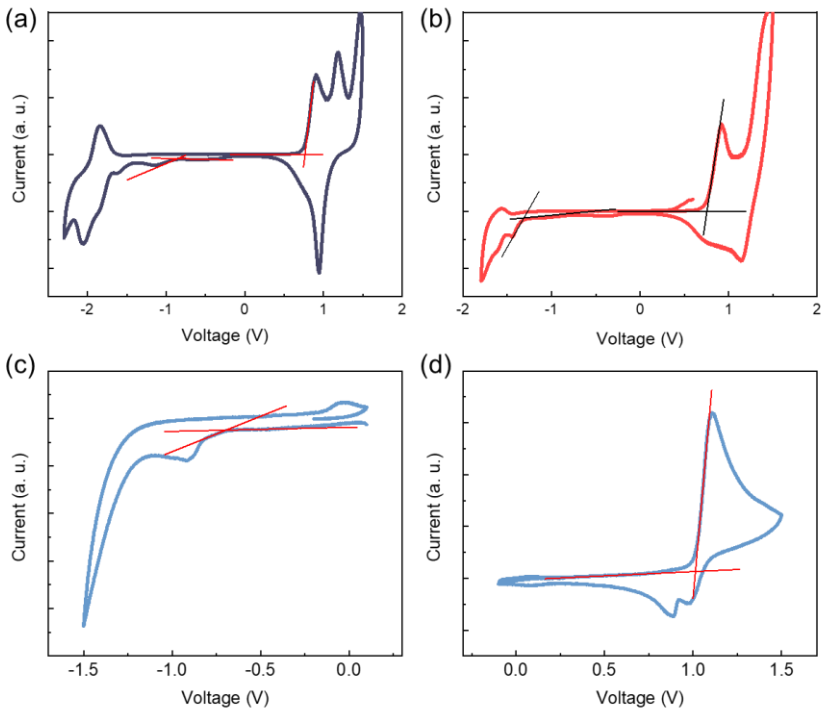

Fig. S2. Cyclic voltammogramms of (a) D18, (b) PM6, and (c-d) L8-BO; (c) reduction and (d) oxdiation cycles.

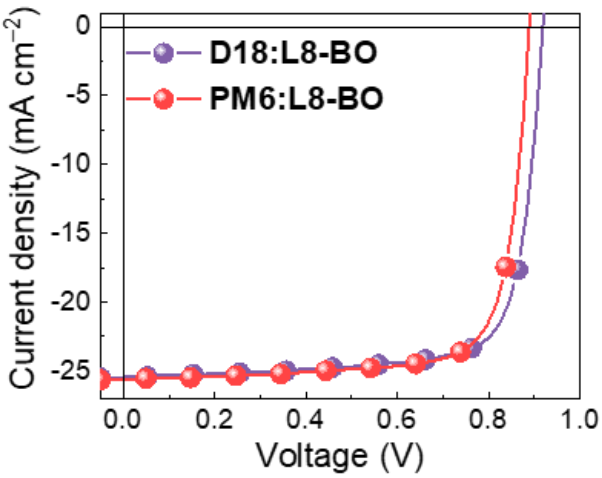

Fig. S3. *J-V* curves of the OSCs based on D18:L8-BO and PM6:L8-BO binary photoactive systems.

Table S2. Photovoltaic parameters of OSCs based on D18:L8-BO and PM6:L8-BO-based photoactive layers.

Photoactive system	V_{OC} **(V)**	J_{SC} **(mA cm^{-2})**	**FF**	**PCE$_{max\ (avg)}$[a] (%)**
D18:L8-BO	0.92	25.47	0.77	18.06 (17.74)
PM6:L8-BO	0.89	25.64	0.78	17.79 (17.41)

[a]Averaged values from 10 independent devices.

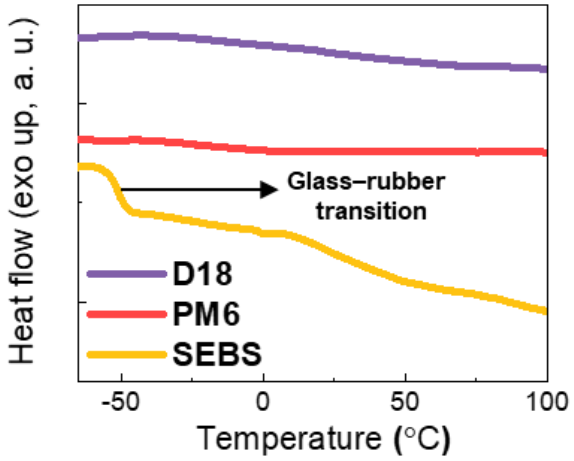

Fig. S4. DSC thermograms in the 2nd heating profiles of D18, PM6, and SEBS.

Table S3. SCLC hole mobility of $D18_{1.0-x}$:$SEBS_x$ blend films at different composition ratios.

System	μ_h ($cm^2\ V^{-1}\ s^{-1}$)[a]
D18	2.8×10^{-4}
$D18_{0.8}$:$SEBS_{0.2}$	2.9×10^{-4}
$D18_{0.6}$:$SEBS_{0.4}$	1.7×10^{-4}
$D18_{0.4}$:$SEBS_{0.6}$	1.0×10^{-4}
$D18_{0.2}$:$SEBS_{0.8}$	2.9×10^{-6}
SEBS	–

[a]Averaged values from 3 independent devices.

Table S4. Tensile properties of $D18_{1.0-x}$:$SEBS_x$ blend films at different composition ratios.

System	*E* (Gpa)	COS (%)	Toughness (MJ m^{-3})
D18	1.6	11	2.1
$D18_{0.8}$:$SEBS_{0.2}$	1.4	14	2.2
$D18_{0.6}$:$SEBS_{0.4}$	1.0	25	3.1
$D18_{0.4}$:$SEBS_{0.6}$	0.4	181	9.8
$D18_{0.2}$:$SEBS_{0.8}$	0.2	>600	>25
SEBS	0.1	>600	>25

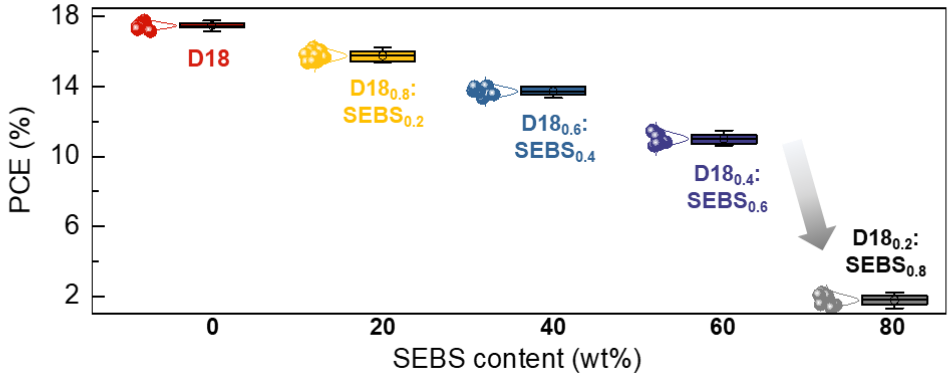

Fig. S5. Gaussian function fitted PCE distributions of OSCs incorporating $D18_{1.0-x}$:$SEBS_x$/L8-BO blend films.

Table S5. SCLC electron and hole mobility of $D18_{0.4}$:$SEBS_{0.6}$/$PM6_x$:L8-$BO_{1.0-x}$ photoactive films.

Bottom Layer	Top Layer	μ_h ($cm^2\ V^{-1}\ s^{-1}$)	μ_e ($cm^2\ V^{-1}\ s^{-1}$)	μ_h/μ_e
$D18_{0.4}$:$SEBS_{0.6}$	**L8-BO**	1.7×10^{-5}	1.8×10^{-4}	0.1
	$PM6_{0.1}$:L8-$BO_{0.9}$	4.7×10^{-5}	1.4×10^{-4}	0.3
	$PM6_{0.3}$:L8-$BO_{0.7}$	1.5×10^{-4}	1.1×10^{-4}	1.3
	$PM6_{0.5}$:L8-$BO_{0.5}$	2.3×10^{-4}	2.0×10^{-5}	11.4
	$PM6_{0.7}$:L8-$BO_{0.3}$	1.4×10^{-4}	3.4×10^{-7}	419
	$PM6_{0.9}$:L8-$BO_{0.1}$	1.6×10^{-4}	5.0×10^{-10}	322700

[a]Averaged values from 3 independent devices.

Table S6. SCLC electron and hole mobility of $PM6_x$:L8-$BO_{1.0-x}$ blend films.

System	μ_h ($cm^2\ V^{-1}\ s^{-1}$)	μ_e ($cm^2\ V^{-1}\ s^{-1}$)
L8-BO	2.7×10^{-7}	1.3×10^{-4}
$PM6_{0.1}$:L8-$BO_{0.9}$	5.3×10^{-5}	1.2×10^{-4}
$PM6_{0.3}$:L8-$BO_{0.7}$	2.7×10^{-4}	1.2×10^{-4}
$PM6_{0.5}$:L8-$BO_{0.5}$	2.4×10^{-4}	9.6×10^{-5}
$PM6_{0.7}$:L8-$BO_{0.3}$	5.4×10^{-4}	2.6×10^{-5}
$PM6_{0.9}$:L8-$BO_{0.1}$	4.9×10^{-4}	4.0×10^{-8}
PM6	4.1×10^{-4}	1.3×10^{-8}

[a]Averaged values from 3 independent devices.

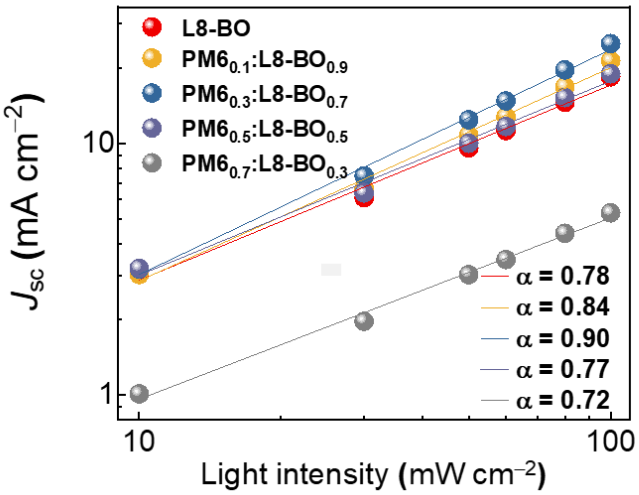

Fig. S6. Light intensity dependent J_{sc} plots of the D18$_{0.4}$:SEBS$_{0.6}$/PM6$_x$:L8-BO$_{1.0-x}$-based OSCs.

Table S7. Tensile properties of D18/L8-BO, D18$_{0.4}$:SEBS$_{0.6}$/L8-BO, and D18$_{0.4}$:SEBS$_{0.6}$/PM6$_{0.3}$:L8-BO$_{0.7}$ photoactive films.

Bottom layer	**Top layer**	***E*** **(Gpa)**	**COS (%)**	**Toughness (MJ m^{-3})**
D18	**L8-BO**	1.9	6	1.4
D18$_{0.4}$:SEBS$_{0.6}$	**L8-BO**	0.9	96	12.1
D18$_{0.4}$:SEBS$_{0.6}$	**PM6$_{0.3}$:L8-BO$_{0.7}$**	0.7	125	15.6

Table S8. PCE and COS values of photoactive systems in previously reported literatures and this study.

Photoactive system	PCE_{max} (%)	COS (%)[a)]	Reference
PM6:IDIC16	4.9	1.4	[5]
PM6:PF2-DTC	8.3	11.3	[5]
PM6:PF2-DTSi	10.8	8.6	[5]
PM6:PF2-DTGe	8.1	6.7	[5]
PTB7:$PC_{71}BM$ (1:1.5)	0.3	2.1	[6]
PTB7:$PC_{71}BM$ (1:1)	0.1	4.3	[6]
PBDTTTPD:$PC_{61}BM$	6.1	0.1	[7]
PTB7-Th:FOIC (BHJ)	11.0	3.1	[8]
PTB7-Th:FOIC (P-i-N)	12.0	11.5	[8]
TQ-F:N2200	7.12	32.6	[9]
TQ-F:N2200:10 wt% PDPS	6.87	50.9	[9]
TQ-F:N2200:20 wt% PDPS	5.43	53.2	[9]
TQ-F:N2200:50 wt% PDPS	3.73	43	[9]
PTB7-Th:P(NDI2HD-T)	5.9	11.6	[10]
PTB7-Th:P(NDI2HD-T):PCBM	6.8	10.7	[10]
PTB7-Th:$PC_{71}BM$	6.0	1.1	[11]
PTB7-Th:ITIC	6.4	3.4	[11]
PTB7-Th:P-15K	3.1	6.0	[11]
PTB7-Th:P-20K	3.4	11.2	[11]
PTB7-Th:P-103K	4.9	22.7	[11]
PTB7-Th:P-163K	5	31.1	[11]
PTB7-Th:$PC_{71}BM$	8.4	1.1	[12]
PBDB-T:Y5-2BO	7.0	2.3	[13]
PBDB-T:P(BDT2BOY5-H)	8.8	19.3	[13]
PBDB-T:P(BDT2BOY5-F)	9.8	16.7	[13]
PBDB-T:P(BDT2BOY5-Cl)	11.1	15.9	[13]
PM6:Y6	15.4	5.8	[14]
PM6:Y6 + 30% PAE	12.4	25.1	[14]
PBDB-T:PYT (BHJ)	14.1	8.5	[15]

PBDB-T:PYT (LbL)	15.2	10.5	[15]
PBDB-T:PNDIHD/DT-0	6.46	20.7	[16]
PBDB-T:PNDIHD/DT-0.41	9.31	30.3	[16]
PBDB-T:PNDIHD/DT-1	6.01	34.5	[16]
PTB7-Th:IEICO-4F	11.4	5	[17]
PTB7-Th:IEICO-4F:5%PDMS	10.8	20	[17]
PTB7-Th:IEICO-4F:10%PDMS	9.2	15	[17]
PTB7-Th:IEICO-4F:15%PDMS	4.9	10	[17]
PM6:N3	15.6	7.1	[18]
PM6:N3:20 wt% $PC_{71}BM$	16.7	9.3	[18]
PM6:N3:50 wt% $PC_{71}BM$	12.7	9	[18]
PM6:N3:80 wt% $PC_{71}BM$	7.1	7.3	[18]
PM6:$PC_{71}BM$	8.3	6.8	[18]
PM6:Y7	15.1	2.3	[19]
PM6-C5:Y7	16.7	12.1	[19]
PM6-C10:Y7	17.0	9.2	[19]
PTzBI:N2200	8.36	15.6	[20]
PTzBI:N2200	4.49	8.1	[20]
PTzBI:N2200	2.92	6.3	[20]
J52:N2200	5.30	19	[21]
PBZ-2Si_L:N2200	4.51	15.5	[21]
PBZ-2Si_M:N2200	6.89	38.1	[21]
PBZ-2Si_H:N2200	6.28	50.2	[21]
PM6:PF2-DTC	8.31	11.3	[5]
PM6:PF2-DTSi	10.77	8.6	[5]
PM6:PF2-DTGe	8.09	6.7	[5]
PBDB-T:PY-O	9.80	9.57	[22]
PBDB-T:PY-S	14.16	8.70	[22]
PBDB-T:PY-T (BHJ)	14.06	8.5	[15]
PBDB-T:PY-T (LBL)	15.17	10.5	[15]
PM6:Y7:N2200 (10 wt%)	15.2	5.58	[23]
PM6:Y7:N2200 (20 wt%)	14.9	10	[23]

PM6:Y7:N2200 (30 wt%)	13.7	11.9	[23]
PM6:Y7:N2200 (40 wt%)	11.4	16.6	[23]
PM6:Y7:N2200 (50 wt%)	8.36	20	[23]
PTQ10:Y6 (BHJ)	14.2	6.6	[23]
PTQ10:Y6 (LbL)	14.4	30.5	[23]
PhAm5:Y7	17.5	13.8	[24]
PhAm10:Y7	16.1	22.6	[24]
PM6:BTP-eC9	15.68	7.0	[25]
PM6:BTP-eC9 + PY-IT 10%	16.52	8.2	[25]
PBDB-T:PYTS-0.0	13.01	18.9	[26]
PBDB-T:PYTS-0.3	14.68	21.6	[26]
PBDB-T:PYTS-1.0	1.71	8.1	[26]
PM6:Y6	14.8	4.5	[27]
PM6:Y6 + BAC 1wt%	14.6	6.2	[27]
PM6:Y6 + BAC 5wt%	14.5	18.0	[27]
PM6:Y6 + BAC 10wt%	13.7	20.0	[27]
PBDB-T:PYBDT	12.6	11.7	[28]
PBDB-T:PYT8T	9.97	3.9	[28]
PBDB-T:PYFS-Ran	12.2	18.1	[28]
PBDB-T:PYFS-Reg	16.1	22.4	[28]
PBDB-T:PYSiO-0	9.83	9.6	[29]
PBDB-T:PYSiO-5	11.4	13.9	[29]
PBDB-T:PYSiO-10	13.5	15.2	[29]
PBDB-T:PYSiO-20	11.9	17.6	[29]
PBDB-T:PYSiO-30	10.7	19.5	[29]
PM6:PY2Se-Cl-o	16.2	11.7	[30]
PM6:PY2Se-Cl-m	1.76	7.03	[30]
PM6:PY2Se-Cl-ran	16.2	17.5	[30]
PM7:L8-BO	16	2.6	[31]
PM7-Thy5:L8-BO	15.4	6.1	[31]
PM7-Thy10:L8-BO	17.1	13.7	[31]
PM6:L8-BO	17.8	2.3	[4]

PM6-*b*-$PDMS_{5k}$:L8-BO	18.2	4.3	[4]
PM6-*b*-$PDMS_{12k}$:L8-BO	18	8.1	[4]
PM6-*b*-$PDMS_{19k}$:L8-BO	17.7	18.1	[4]
PM6:FDY-m-TAT	18.07	18.23	[32]
D18:MYT	16.53	1.3	[33]
D18:TYT-L	17.47	6.4	[33]
D18:TYT-S	18.61	21.6	[33]
PBQx-TF:MYBT	15.85	10.3	[34]
PBQx-TF:DYBT-C0	17.18	17.3	[34]
PBQx-TF:DYBT-C4	18.26	31.8	[34]
PBQx-TF:DYBT-C8	16.22	28.0	[34]
D18: :L8-BO	18.11	1.5	[3]
$D18_{0.8}$-*r*-$PEHDT_{0.2}$:L8-BO	15.34	10.4	[3]
$D18_{0.8}$-*s*-$PEHDT_{0.2}$:L8-BO	19.03	17.2	[3]
$D18_{0.8}$:$PEHDT_{0.2}$:L8-BO	16.41	5.6	[3]
PEHDT:L8-BO	5.03	30.7	[3]
PNTB6-Cl:BTP-C3	13.6	53.0	[35]
PNTB6-Cl:BTP-Si6	16.5	79.2	[35]
PNTB6-Cl:BTP-Si8	13.5	85.2	[35]
PNTB6-Cl:BTP-Si4	16.4	95.5	[35]
PNTB6-Cl:BTP-C3	13.6	53.0	[35]
D18/L8-BO	17.48	8	[36]
D180.8:SEBS0.2/L8-BO	17.40	12	[36]
D180.6:SEBS0.4/L8-BO	15.22	17	[36]
D180.4:SEBS0.6/L8-BO	12.13	126	[36]
PM6:BTP-eC9	18.44	4.6	[37]
PM6-$Cl_{0.2}$-*r*-D18-$Cl_{0.8}$-TCl:BTP-eC9	17.07	10.11	[37]
PM6-$Cl_{0.8}$-b-D18-$Cl_{0.2}$-TCl:BTP-eC9	18.55	22.58	[37]
PM6-$Cl_{0.5}$-b-D18-$Cl_{0.5}$-TCl:BTP-eC9	17.58	17.75	[37]
PM6-$Cl_{0.2}$-b-D18-$Cl_{0.8}$-TCl:BTP-eC9	17.25	16.71	[37]
PM6-$Cl_{0.8}$-b-D18-$Cl_{0.2}$-BTB:BTP-eC9	15.37	25.38	[37]

PM6-$Cl_{0.8}$-b-D18-$Cl_{0.2}$-BTB:PM6:BTP-eC9	19.57	11.03	[37]
D18:BTP-C3	16.8	19.2	[38]
D18:BTP-EH	17.9	25.2	[38]
D18:BTP-HD	15.5	30.39	[38]
PBQx-TF:PYIT	15.6	16.5	[39]
PBQx-TF:P1:PYIT	16.4	19.5	[39]
PBQx-TF:P2:PYIT	17.1	20.4	[39]
PM6:BTP-eC9	17.63	5.4	[40]
PM6:BTP-eC9:2Qx-C3	18.79	15	[40]
PM6-*b*-PYSe	12.33	7.47	[41]
D18/BTP-eC9	17.57	9.67	[41]
D18/PM6-*b*-PYSe/BTP-eC9	17.97	17.69	[41]
PM6:DY-FBrL	18.75	18.54	[42]
PM6:PDY-FL	14.13	23.45	[42]
PBDB-TF:MYBO	17.57	2	[43]
PBET-TF:MYBO	17.76	31	[43]
D18/Y6	15.71	10.56	[44]
D18/Y6:SEBS	16.54	26.38	[44]
PBDB-T:PY-EH	10.85	11.15	[45]
PBDB-T:PY-SiO	12.04	18.32	[45]
PM6-$Cl_{0.8}$-*b*-D18-$Cl_{0.2}$-BTD:BTP-eC9	18.09	31.29	[46]
PM6-$Cl_{0.5}$-*b*-D18-$Cl_{0.5}$-BTD:BTP-eC9	17.33	28.28	[46]
PM6:N3	15.42	6.9	[47]
PM6:N3 + SEBS 2%	15.98	8.1	[47]
PM6:N3 + SEBS 5%	15.57	9.5	[47]
PM6:N3 + SEBS 10%	14.42	11.2	[47]
PM6:N3 + SEBS 20%	13.10	11.9	[47]
PM6:N3 + SEBS 30%	11.55	13.0	[47]
PM6:PYFT-*o*	15.23	4.7	[48]
PM6:PYFT-*o* + SEBS 4.8%	14.27	5.8	[48]
PM6:PYFT-*o* + SEBS 9.1%	13.79	7.8	[48]

PM6:PYFT-*o* + SEBS 16.7%	12.70	10.2	[48]
PM6:PYFT-*o* + SEBS 23.1%	12.23	16.9	[48]
PM6:PYFT-*o* + SEBS 33.3%	11.48	26.2	[48]
PM6:PYFT-*o* + SEBS 41.2%	10.16	51.8	[48]
PM6:PYFT-*o* + SEBS 50.0%	8.04	67.3	[48]
PM6:PYFT-*o* + SEBS 60.0%	4.54	98.3	[48]
$D18_{0.4}$:$SEBS_{0.6}$/$PM6_{0.3}$:L8-$BO_{0.7}$	**15.69**	**125**	**This study**

[a] The presented COSs stand for the values measured by pseudo free-standing tensile test.

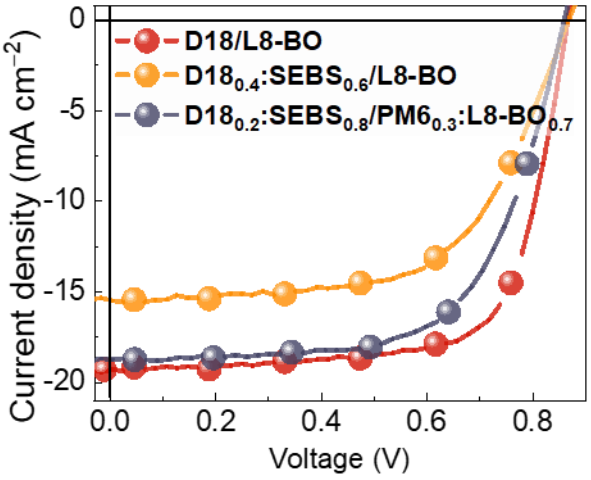

Fig. S7. *J-V* curves of the IS-OSCs basd on D18/L8-BO, $D18_{0.4}$:$SEBS_{0.6}$/L8-BO, and $D18_{0.4}$:$SEBS_{0.6}$/$PM6_{0.3}$:L8-$BO_{0.7}$ photoactive films.

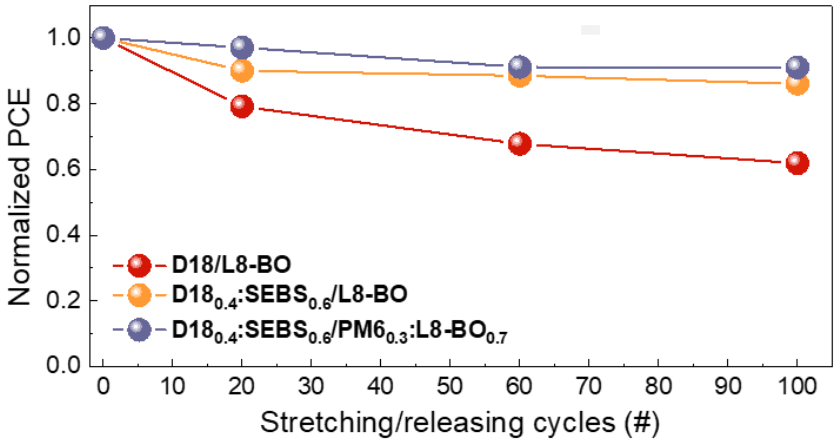

Fig. S8. Normalized PCE of IS-OSCs during repeated stretching and releasing cycles at a fixed strain of 10%.

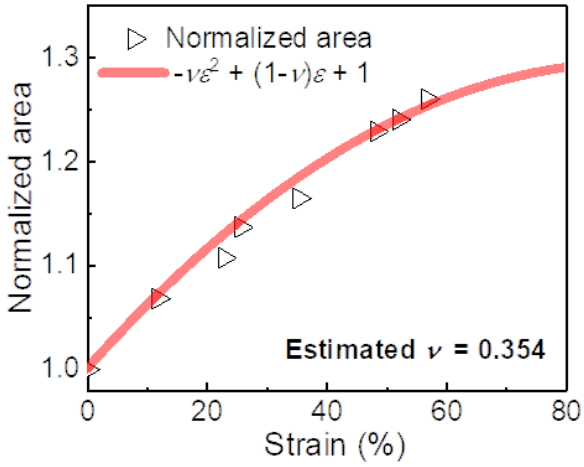

Fig. S9. Changes in the photoactive area of the IS-OSCs in terms of engineering strain. The plot is used to estimate the υ value by quadratic function fitting.

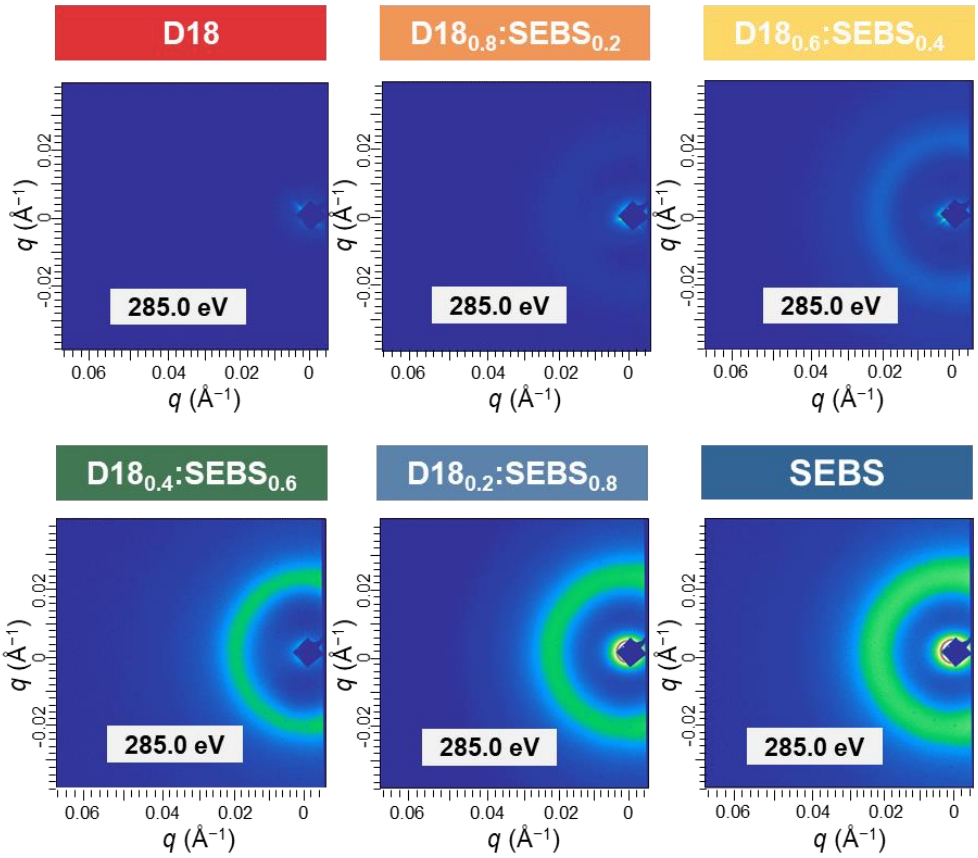

Fig. S10. RSoXS 2D-image of D18$_{1.0-x}$:SEBS$_x$ blend films at different composition ratios.

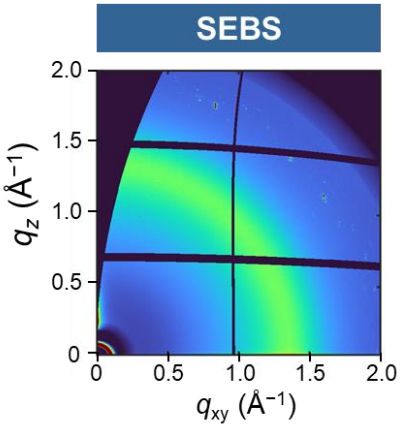

Fig. S11. GIXS 2D-image of SEBS.

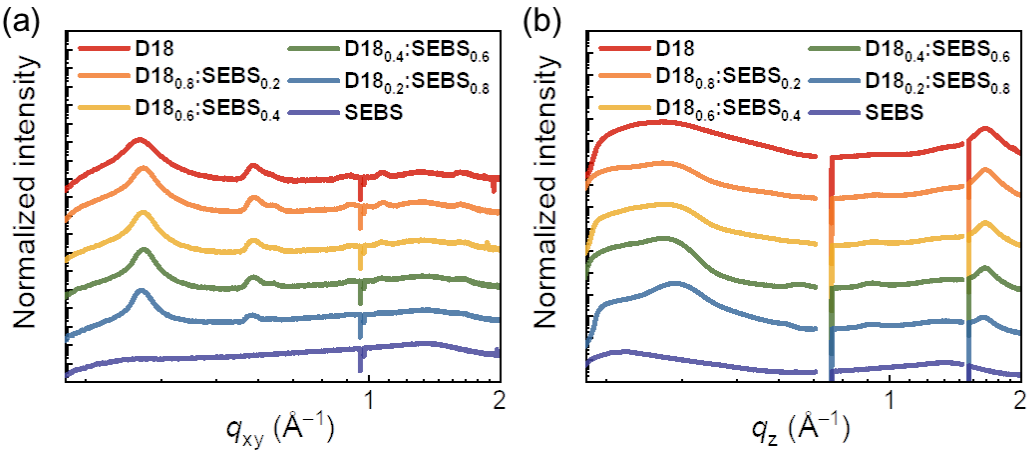

Fig. S12. GIXS linecut profiles of $D18_{1.0-x}$:$SEBS_x$ thin films in the (a) IP and (b) OOP directions.

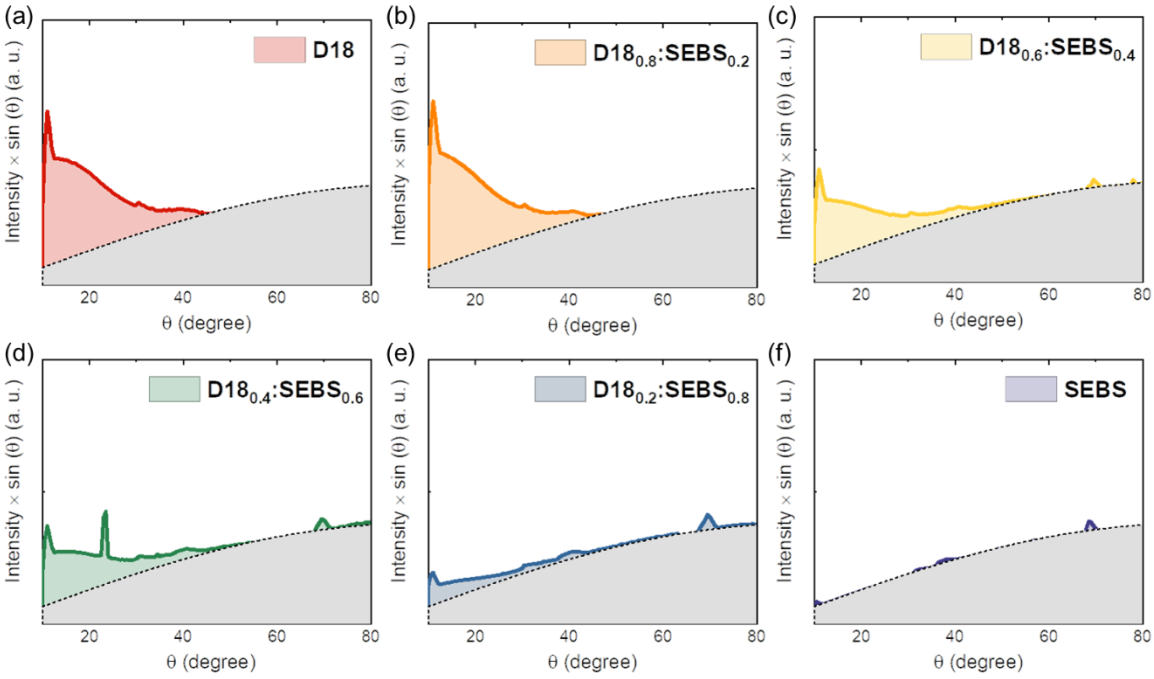

Fig. S13. Pole figures for GIXS (010) scattering peaks (q range of 1.5 – 1.8 Å^{-1}) of (a) D18, (b) $D18_{0.8}$:$SEBS_{0.2}$, (c) $D18_{0.6}$:$SEBS_{0.4}$, and (d) $D18_{0.4}$:$SEBS_{0.6}$, (e) $D18_{0.2}$:$SEBS_{0.8}$, and (f) SEBS thin films.

Table S9. Crystalline parameters of $D18_{1.0-x}$:$SEBS_x$ blend films estimated from GIXS profiles.

P_D:elastomer	$L_{c\ (010)}^{OOP}$ (nm)	*r*-DoC $_{D18(010)}$ / N_{D18}
D18	4.37	0.84
$D18_{0.8}$:$SEBS_{0.2}$	4.85	1.05
$D18_{0.6}$:$SEBS_{0.4}$	4.77	0.84
$D18_{0.4}$:$SEBS_{0.6}$	4.68	0.85
$D18_{0.2}$:$SEBS_{0.8}$	3.81	0.32
SEBS	–	–

Table S10. Molar fractions of D18 and SEBS in $D18_{1.0-x}$:$SEBS_x$ blend films, which were estimated based on the M_n values.

P_D:elastomer	N_{D18} [a]	N_{SEBS} [a]
D18	1.00	0.00
$D18_{0.8}$:$SEBS_{0.2}$	0.91	0.09
$D18_{0.6}$:$SEBS_{0.4}$	0.80	0.20
$D18_{0.4}$:$SEBS_{0.6}$	0.64	0.36
$D18_{0.2}$:$SEBS_{0.8}$	0.40	0.60
SEBS	0.00	1.00

[a]Molar fraction of D18 and SEBS in $D18_x$:$SEBS_{1.0-x}$ blend films.

Table S11. The $I_{(0\text{-}0)}/ I_{(0\text{-}1)}$ obtained from UV-Vis absorption spectra of $D18_{1.0\text{-}x}$:$SEBS_x$ films.

***P*D:elastomer**	$I_{(0\text{-}0)}/ I_{(0\text{-}1)}$
D18	1.19
$D18_{0.9}$:$SEBS_{0.1}$	1.22
$D18_{0.8}$:$SEBS_{0.2}$	1.24
$D18_{0.7}$:$SEBS_{0.3}$	1.26
$D18_{0.6}$:$SEBS_{0.4}$	1.27
$D18_{0.5}$:$SEBS_{0.5}$	1.28
$D18_{0.4}$:$SEBS_{0.6}$	1.30

References

1. F. Lin, C. Wu and D. Cui, *J. Polym. Sci. Part A: Polym. Chem.*, 2017, **55**, 1243-1249.
2. Z. H. Wu, C. Sun, S. Dong, X. F. Jiang, S. P. Wu, H. B. Wu, H. L. Yip, F. Huang and Y. Cao, *J. Am. Chem. Soc.*, 2016, **138**, 2004-2013.
3. J.-W. Lee, H.-G. Lee, E. S. Oh, S.-W. Lee, T. N.-L. Phan, S. Li, T.-S. Kim and B. J. Kim, *Joule*, 2024, **8**, 204-223.
4. S. Seo, J.-W. Lee, D. J. Kim, D. Lee, T. N.-L. Phan, J. Park, Z. Tan, S. Cho, T.-S. Kim and B. J. Kim, *Adv. Mater.*, 2023, **35**, 2300230.
5. Q. P. Fan, W. Y. Su, S. S. Chen, W. Kim, X. B. Chen, B. Lee, T. Liu, U. A. Mendez-Romero, R. J. Ma, T. Yang, W. L. Zhuang, Y. Li, Y. W. Li, T. S. Kim, L. T. Hou, C. Yang, H. Yan, D. H. Yu and E. G. Wang, *Joule*, 2020, **4**, 658-672.
6. J. H. Kim, J. Noh, H. Choi, J. Y. Lee and T. S. Kim, *Chem. Mater.*, 2017, **29**, 3954-3961.
7. T. Kim, J. H. Kim, T. E. Kang, C. Lee, H. Kang, M. Shin, C. Wang, B. W. Ma, U. Jeong, T. S. Kim and B. J. Kim, *Nat. Commun.*, 2015, **6**.
8. Y. L. Wang, Q. L. Zhu, H. B. Naveed, H. Zhao, K. Zhou and W. Ma, *Adv. Energy Mater.*, 2020, **10**.
9. S. Chen, S. Jung, H. J. Cho, N.-H. Kim, S. Jung, J. Xu, J. Oh, Y. Cho, H. Kim, B. Lee, Y. An, C. Zhang, M. Xiao, H. Ki, Z.-G. Zhang, J.-Y. Kim, Y. Li, H. Park and C. Yang, *Angew. Chem. Int. Ed.*, 2018, **57**, 13277-13282.
10. W. Lee, J.-H. Kim, T. Kim, S. Kim, C. Lee, J.-S. Kim, H. Ahn, T.-S. Kim and B. J. Kim, *J. Mater. Chem. A*, 2018, **6**, 4494-4503.
11. J. Choi, W. Kim, S. Kim, T. S. Kim and B. J. Kim, *Chem. Mater.*, 2019, **31**, 9057-9069.
12. W. Lee, J. H. Kim, T. Kim, S. Kim, C. Lee, J. S. Kim, H. Ahn, T. S. Kim and B. J. Kim, *J. Mater. Chem. A*, 2018, **6**, 4494-4503.
13. J. W. Lee, C. Sun, B. S. Ma, H. J. Kim, C. Wang, J. M. Ryu, C. Lim, T. S. Kim, Y. H. Kim, S. K. Kwon and B. J. Kim, *Adv. Energy Mater.*, 2021, **11**.
14. J. H. Han, F. Bao, D. Huang, X. C. Wang, C. M. Yang, R. Q. Yang, X. G. Jian, J. Y. Wang, X. C. Bao and J. H. Chu, *Adv. Funct. Mater.*, 2020, **30**.
15. Q. Wu, W. Wang, Y. Wu, Z. Chen, J. Guo, R. Sun, J. Guo, Y. Yang and J. Min, *Adv. Funct. Mater.*, 2021, **31**, 2010411.
16. J.-W. Lee, N. Choi, D. Kim, T. N.-L. Phan, H. Kang, T.-S. Kim and B. J. Kim, *Chem. Mater.*, 2021, **33**, 1070-1081.
17. Z. Wang, M. Xu, Z. Li, Y. Gao, L. Yang, D. Zhang and M. Shao, *Adv. Funct. Mater.*, 2021, **31**, 2103534.
18. Z. Peng, K. Jiang, Y. Qin, M. Li, N. Balar, B. T. O'Connor, H. Ade, L. Ye and Y. Geng, *Adv. Energy Mater.*, 2021, **11**, 2003506.
19. J. W. Lee, D. Jeong, D. J. Kim, T. N. L. Phan, J. S. Park, T. S. Kim and B. J. Kim, *Energy Environ. Sci.*, 2021, **14**, 4067-4076.

20. B. J. Lin, L. Zhang, H. Zhao, X. B. Xu, K. Zhou, S. Zhang, L. Gou, B. B. Fan, L. Zhang, H. P. Yan, X. D. Gu, L. Ying, F. Huang, Y. Cao and W. Ma, *Nano Energy*, 2019, **59**, 277-284.
21. M. Xu, D. Zhang, Z. Wang, Z. Liu, X. Gao, J. He, Y. Gao, Z. Li and M. Shao, *Chem. Eng. J.*, 2022, **440**, 135829.
22. Q. Wu, W. Wang, Y. Wu, R. Sun, J. Guo, M. M. Shi and J. Min, *Natl. Sci. Rev.*, 2022, **9**, nwab151.
23. J.-W. Lee, G.-U. Kim, D. J. Kim, Y. Jeon, S. Li, T.-S. Kim, J.-Y. Lee and B. J. Kim, *Adv. Energy Mater.*, 2022, **12**, 2200887.
24. J.-W. Lee, S. Seo, S.-W. Lee, G.-U. Kim, S. Han, T. N.-L. Phan, S. Lee, S. Li, T.-S. Kim, J.-Y. Lee and B. J. Kim, *Adv. Mater.*, 2022, **34**, 2207544.
25. W. Song, K. Yu, J. Ge, L. Xie, R. Zhou, R. Peng, X. Zhang, M. Yang, Z. Wei and Z. Ge, *Matter*, 2022, **5**, 1877-1889.
26. Z. Genene, J.-W. Lee, S.-W. Lee, Q. Chen, Z. Tan, B. A. Abdulahi, D. Yu, T.-S. Kim, B. J. Kim and E. Wang, *Adv. Mater.*, 2022, **34**, 2107361.
27. Z. Wang, D. Zhang, M. Xu, J. Liu, J. He, L. Yang, Z. Li, Y. Gao and M. Shao, *Small*, 2022, **18**, 2201589.
28. J.-W. Lee, C. Sun, S.-W. Lee, G.-U. Kim, S. Li, C. Wang, T.-S. Kim, Y.-H. Kim and B. J. Kim, *Energy Environ. Sci.*, 2022, **15**, 4672-4685.
29. J.-W. Lee, S.-W. Lee, J. Kim, Y. H. Ha, C. Sun, T. Ngoc-Lan Phan, S. Lee, C. Wang, T.-S. Kim, Y.-H. Kim and B. J. Kim, *J. Mater. Chem. A*, 2022, **10**, 20312-20322.
30. Q. Fan, R. Ma, W. Su, Q. Zhu, Z. Luo, K. Chen, Y. Tang, F. R. Lin, Y. Li, H. Yan, C. Yang, A. K.-Y. Jen and W. Ma, *Carbon Energy*, 2023, **5**, e267.
31. Q. Wan, S. Seo, S.-W. Lee, J. Lee, H. Jeon, T.-S. Kim, B. J. Kim and B. C. Thompson, *J. Am. Chem. Soc.*, 2023, **145**, 11914-11920.
32. Y. Ding, W. A. Memon, D. Zhang, Y. Zhu, S. Xiong, Z. Wang, J. Liu, H. Li, H. Lai, M. Shao and F. He, *Angew. Chem. Int. Ed.*, 2024, **63**, e202403139.
33. J.-W. Lee, C. Sun, J. Lee, D. J. Kim, W. J. Kang, S. Lee, D. Kim, J. Park, T. N.-L. Phan, Z. Tan, F. S. Kim, J.-Y. Lee, X. Bao, T.-S. Kim, Y.-H. Kim and B. J. Kim, *Adv. Energy Mater.*, 2024, **14**, 2303872.
34. J.-W. Lee, C. Sun, S. Lee, D. J. Kim, E. S. Oh, T. N.-L. Phan, T. H.-Q. Nguyen, S. Seo, Z. Tan, M. J. Lee, J.-Y. Lee, X. Bao, T.-S. Kim, C. Lee, Y.-H. Kim and B. J. Kim, *Nano Energy*, 2024, **125**, 109541.
35. Z. Wang, D. Zhang, L. Yang, O. Allam, Y. Gao, Y. Su, M. Xu, S. Mo, Q. Wu, Z. Wang, J. Liu, J. He, R. Li, X. Jia, Z. Li, L. Yang, M. D. Weber, Y. Yu, X. Zhang, T. J. Marks, N. Stingelin, J. Kacher, S. S. Jang, A. Facchetti and M. Shao, *Science*, 2025, **387**, 381-387.
36. J.-W. Lee, T. H.-Q. Nguyen, E. S. Oh, S. Lee, J. Choi, H. S. Kwon, C. Wang, S. Lee, J.-Y. Lee, T.-S. Kim and B. J. Kim, *Adv. Energy Mater.*, 2024, **14**, 2401191.
37. C. Lin, Z. Chen, R. Peng, W. Song, J. Gao, X. Yu, T. Feng, Y. Bai and Z. Ge, *Energy Environ. Sci.*, 2024, **17**, 9359-9374.

38. D. Zhang, J. Liu, X. Gao, Z. Wang, J. He, Z. Wang, L. Yang, Y. Gao and M. Shao, *Energy Environ. Sci.*, 2025, **18**, 2342-2352.
39. G.-U. Kim, C. Choi, D. Jeong, D. J. Kim, T. N.-L. Phan, S. Song, J. Park, T.-S. Kim, Y.-H. Kim and B. J. Kim, *Adv. Energy Mater.*, 2023, **13**, 2302125.
40. S. You, Y. Zhang, B. Huang, S. Y. Jeong, X. Shuai, S. Huang, H. Y. Woo, F. Wu and L. Chen, *Adv. Funct. Mater.*, 2025, **35**, 2414803.
41. D. Zhang, Y. Wu, C. Yan, P. Cheng, G. Zhang, H. Yang and C. Cui, *Adv. Funct. Mater.*, 2024, **34**, 2407681.
42. Y. Ding, S. Xiong, W. A. Memon, D. Zhang, Z. Wang, M. Li, Z. Deng, H. Li, M. Shao and F. He, *Angew. Chem. Int. Ed.*, 2025, DOI: https://doi.org/10.1002/anie.202421430, e202421430.
43. J.-W. Lee, E. S. Oh, S. Lee, T. N.-L. Phan, T.-S. Kim, J.-Y. Lee, J. R. Reynolds and B. J. Kim, *Joule*, 2025, **9**, 101792.
44. W. Tang, Z. Ding, Y. Su, Q. Weng, Y. Zhang, R. Li, W. Huang, Z. Wang, Y. Wu, Y. Han, K. Zhao, Z. Yang, X. Wang and S. Liu, *Adv. Funct. Mater.*, 2024, **34**, 2312289.
45. J. He, D. Zhang, J. Liu, l. Yang, Y. Gao and M. Shao, *ACS Appl. Mater. Interfaces*, 2024, **16**, 22294-22302.
46. C. Lin, R. Peng, W. Song, J. Gao, T. Feng, Y. Bai, Q. Liu, M. Yang, J. Zhang and Z. Ge, *Angew. Chem. Int. Ed.*, 2025, **64**, e202420121.
47. Z. Peng, K. Xian, Y. Cui, Q. Qi, J. Liu, Y. Xu, Y. Chai, C. Yang, J. Hou, Y. Geng and L. Ye, *Adv. Mater.*, 2021, **33**, 2106732.
48. S. Li, M. Gao, K. Zhou, X. Li, K. Xian, W. Zhao, Y. Chen, C. He and L. Ye, *Adv. Mater.*, 2024, **36**, 2307278.